Journal of Nuclear Medicine, published on November 21, 2018 as doi:10.2967/jnumed.118.216721

MEK inhibition induces therapeutic iodine uptake in a murine model of anaplastic thyroid cancer.

Oussama ElMokh[1], Vincent Taelman[2], Piotr Radojewski[2], Matthias A. Roelli[1], Amandine Stoss[1], Rebecca A. Dumont[3], Matthias S. Dettmer[4], Wayne A. Phillips[5], Martin A. Walter[2], and Roch-Philippe Charles[1*]

[1]Institute for Biochemistry and Molecular Medicine, University of Bern, Switzerland
[2]Institute for Nuclear Medicine, Geneva University Hospitals, Switzerland
[3]Department of Radiology, University of California at San Francisco, USA
[4]Institute for Pathology, University of Bern, Switzerland
[5]Cancer Biology Laboratory, Peter MacCallum Cancer Centre, Melbourne, Australia

*Corresponding author:
Roch-Philippe Charles (PhD)
Institute for Biochemistry and Molecular Medicine, University of Bern,
Bühlstrasse 28, CH-3012 Bern, Switzerland.
Phone: +41 31 631 4344 Email: roch-philippe.charles@ibmm.unibe.ch

First author:
Oussama ElMokh
Central Laboratory of Hematology, University Hospital of Lausanne (CHUV),
27-Sud, Rue du Bugnon, CH-1011 Lausanne, Switzerland.
Phone: +41 21 314 4214 Email: oussama.el-mokh@chuv.ch

Funding support: Swiss National Science Foundation grant 31003A_149824/1 and Swiss National Science Foundation grant NCCR-TransCure.

Conflict of interest: The authors declare no potential conflicts of interest relevant to this article.

Word count (total): 4958

Running title: MEKi induces 131I uptake in advanced thyroid cancer.

ABSTRACT

Rationale: Anaplastic thyroid carcinoma (ATC) is refractory to radioiodine therapy in part due to impaired iodine metabolism. We targeted the MAPK and PI3'K pathways with the intent to induce radioiodine uptake for radioiodine treatment of ATC.

Methods: Human ATC cells were used to evaluate the ability of pharmacological inhibition of the mitogen-activated protein kinase and phosphatidylinositol 3-kinase pathways to induce radioiodine uptake. Thyrocyte-specific double mutant $BRAF^{V600E}$ $PIK3CA^{H1047R}$ mice were treated with a MEK inhibitor followed by radioiodine treatment and tumor burden was monitored by ultrasound imaging.

Results: ATC cell lines showed an increase in sodium-iodine symporter transcription when treated with a MEK or $BRAF^{V600E}$ inhibitor alone and in combination with PI3'K inhibitor. This translated into a dose-dependent elevation of iodine uptake following treatment with a MEK inhibitor alone and in combination with a PI3'K inhibitor. *In vivo*, MEK inhibition but not BRAF nor PI3'K inhibition upregulated sodium-iodine symporter transcription. This translated into a stable reduction of tumor burden when mice were treated with a MEK inhibitor prior to radioiodine administration.

Conclusion: This study confirms the ability of MEK inhibition to induce iodine uptake in *in vitro* and *in vivo* models of ATC. The approach of using a MEK inhibitor before radioiodine treatment could readily be translated into clinical practice and provide a much-needed therapeutic option for patients with ATC.

Key words: Drug resistance, NIS, Targeted therapy, differentiation.

INTRODUCTION

Anaplastic thyroid carcinoma (ATC) is one of the most aggressive human malignancies (*1*,*2*) and is refractory to radioiodine therapy (*3*).

Impaired iodine metabolism can result from dysregulation of the mitogen-activated protein kinase (MAPK) and phosphatidylinositol 3-kinase (PI3'K) pathways (Figure 1), which regulate a variety of cellular activities and have been implicated in the development of various human cancers (*4*). MAPK mutations are common in ATC, with 25% of tumors harboring KRAS mutations and depending on the study 27% to 45% are carrying BRAF mutations (*5*–*7*). The most common mutation found in BRAF codes for the protein kinase $BRAF^{V600E}$, which induces constitutive activation of the downstream pathway (Figure 1). Several important PI3'K pathway mutations in ATC include *PTEN* deletions (10-20%) and *PIK3CA* mutations (15-25%) (*8*). We have previously shown that the $BRAF^{V600E}$ mutation in combination with the $PIK3CA^{H1047R}$ mutation induces tumor progression from PTC to ATC in a mouse model (*9*).

The link between alterations of the MAPK and PI3'K pathways and impairment of iodine metabolism is well-documented, although the underlying mechanisms not fully elucidated. BRAF mutations are associated with impairment of NIS function and subsequent increased resistance to radioiodine uptake in (*10*,*11*) thyroid cancers. Some studies suggest that BRAF inhibits the expression of PAX8 and prevents transcription of *NIS* (*12*).

The relationship between the MAPK pathway and the ability to store iodine intracellularly has been further demonstrated in mouse models of papillary thyroid cancer (PTC), where selective MAPK pathway antagonists have been shown to increase the expression of NIS with resultant increased uptake of iodine (*13*). Inhibition of the MAPK pathway via MEK is a promising strategy for treatment of iodine refractory thyroid cancers and, specifically, ATC. Several studies

suggest that PI3'K inhibition increases radioiodine uptake in thyroid cancer cells (*14*,*15*), however this has not yet been evaluated *in vivo*. In this study, we aimed to investigate the consequences of pharmacologically targeting the MAPK and PI3'K pathways separately and in combination to induce radioiodine uptake in ATC cell lines and in a lethal double mutant ATC ($BRAF^{V600E}$ $PIK3CA^{H1047R}$) mouse model. We hypothesized that pharmacological restoration of radioiodine uptake with subsequent RAI would be an effective means of therapy in a murine model of ATC.

MATERIALS AND METHODS

Small Molecule Kinases Inhibitors

Inhibitors, PD-325901 (MEK1/2), PLX-4032/vemurafenib ($BRAF^{V600E}$), PLX-4720 ($BRAF^{V600E}$) and GDC-0941 (class I PI3'K) were purchased from Abmole Bioscience, Hong-Kong. PLX-4032 was used *in vitro* as a $BRAF^{V600E}$ inhibitor but due to poor solubility (*16*), PLX-4720 was used for *in vivo* experiments.

$BRAF^{V600E}$ $PIK3CA^{H1047R}$ Mice

Transgenic mice were bred by combining the following alleles: $Braf^{CA}$ (*17*), $Pik3ca^{Lat}$ (*18*) and $Thyro::Cre^{ERT2}$ (*19*) as previously described (*9*). Mutations were induced by 5 consecutive daily injections of 1 mg tamoxifen IP. Mice were cared for in accordance with Swiss federal guidelines, housed in isolated ventilated cages and fed ad libitum in a 12/12 h cycle of light and dark. The experimental protocol was approved by the Bernese cantonal ethical commission for animal experimentation (License number: BE120/13).

Cell Lines

The human cell lines 8505c, Sw1736 and OCUT-2 were obtained and maintained as described previously (*20*).

In Vitro Evaluation of ATC *NIS* mRNA Expression

Cells were seeded in 10 cm Petri dishes at 25% confluency overnight then treated with PD-325901 at 10 nM, GDC-0941 at 100 nM, PLX-4032 at 100 nM, PD-325901 at 10 nM with GDC-0941 at 100 nM or PLX-4032 at 100 nM with GDC-0941 at 100 nM at 37 °C for 48 h. Cells were

washed twice with 5 ml cold PBS then collected in 1 ml by scrapping the dish surface. A centrifugation for 10 min at 3'000 g was performed and the cell pellets were frozen in liquid nitrogen then stored at -80 °C. *NIS* mRNA levels were evaluated by quantitative PCR see below.

In Vivo Evaluation of Thyroid-Specific Gene Expression Following Kinase Inhibition

Thyroid tissues from 8 single mutant $BRAF^{V600E}$ mice (*Braf*$^{CA/+}$*; Thyro::Cre*^{ERT2}) treated for 21 days with 12.5 mg/kg PD-325901 (N=4) or Hydroxypropyl methylcellulose 0.5%, Tween-80 0.2% was used as a control (N=4) by oral gavage were fixed in formalin and embedded in paraffin blocks (*21*), from which RNA was extracted with High Pure FFPET RNA isolation kit (Roche) according to the manufacturer's protocol.

23 $BRAF^{V600E}$ $PIK3CA^{H1047R}$ double mutant mice (*Braf*$^{CA/+}$*; Pik3ca*$^{Lat/+}$*; Thyro::Cre*^{ERT2}) were treated 2 months after tumor induction with PD-325901 at 5 mg/kg (n=4), PLX-4720 at 30 mg/kg (n=5) or GDC-0941 at 50 mg/kg (n=5) as single treatments, or PLX/GDC (n=5) and PD/GDC (n=4) in combination by oral gavage daily for 10 days. Additionally, thyroid glands from 12 Cre negative mice (*Braf*$^{CA/+}$*; Pik3ca*$^{Lat/+}$) were combined for a total of n=3 and used as non-tumoral controls. Hydroxypropyl methylcellulose 0.5%, Tween-80 0.2% was used as a control. Mice were then sacrificed, thyroid glands were dissected and snap frozen using liquid nitrogen, and total RNA was purified with the QIAzol reagent from Qiagen according to the manufacturer's instructions with a TissueLyser LT using iron beads. *Nis, Tshr, Tg, Pax8, Tpo* and *Ttf1* mRNA levels were evaluated (see below).

Quantitative PCR

500 ng of RNA underwent reverse transcription using Oligo(dT)12-18 Primer and the Super Script II Reverse Transcriptase from Invitrogen following the manufacturer's suggested protocol. Samples were run on ViiA™ 7 Real-Time PCR System (Applied Biosystems, Life Technologies) using the TaqMan® gene expression Master Mix and primers from Applied Biosystems. GAPDH was used for normalization using the $2^{\Delta\Delta Ct}$ calculation method. All values were expressed as percent of the baseline transcription levels found in non-tumoral Cre negative thyroid tissues. The following primers were purchased from Applied Biosystems, Life Technologies: *NIS* (Hs00166567_m1), *Nis* (Mm01351811_m1), *Tg* (Mm01200340_m1), *Ttf1* (Mm00657018_m1), *Pax8* (Mm00440623_m1), *Tpo* (Mm00456355_m1), *Tshr* (Mm00442027_m1), *GAPDH* (Hs02758991_g1) and *Gapdh* (Mm99999915_g1).

In Vitro ^{123}I Uptake Assay

Cells were seeded in Corning® 96-wells plates at 30% confluency, incubated overnight at 37°C and 5% CO_2, and treated for 48 h with various concentrations of PD-325901 (0, 0.1, 1, 10, 100 and 1000 nM) with or without 200 nM of GDC-0941. All except for one of the PD-325901 concentrations used were below the Cmax value (200 nM), which corresponds to the maximal concentration in human plasma without toxicity recorded (*22*). Cell were washed with PBS and cell viability was assessed with the AlamarBlue® Cell Viability Reagent (#765506, Invitrogen) by measuring fluorescence at 634 nm (SpectraMax M4 plate reader, Molecular Devices, USA). After removal of AlamarBlue®, cells were washed with PBS and incubated with culture medium containing 18.5 kBq of ^{123}I (GE Healthcare, Switzerland) for 1 h at 37 °C. Then the medium was removed and the cells were washed 3 times with PBS, then replaced by 50 µl of scintillation

reagent (MicroScint-20, PerkinElmer) per well. Activity was measured with a microplate scintillation counter (Packard Topcount NXT).

In Vivo ^{125}I Uptake Assay

11 BRAF^{V600E} PIK3CA^{H1047R} double mutant mice were treated daily by oral gavage for 2 weeks with control (n=4), PD-325901 at 5 mg/kg alone (n=4) or in combination with GDC-0941 at 30 mg/kg (n=3). Hydroxypropyl methylcellulose with 0.5% Tween80 was used as a control. Then, mice were injected via tail vein with 1.11 MBq of ^{125}I (ANAWA, Biomedical Services & Products, Switzerland) and euthanized 1 h later with CO_2. Thyroid glands, salivary glands, liver and blood were harvested and weighed. Radioactivity was quantified for 30 seconds per sample using a PerkinElmer 2470 automatic gamma counter.

In Vivo Tumor Treatment Experiment

16 BRAF^{V600E} PIK3CA^{H1047R} double mutant mice were treated daily by oral gavage for 10 days with control (n=8) or PD-325901 at 5 mg/kg (n=8). Following this, half of the mice in each group were injected with 18.5 MBq of ^{131}I (PerkinElmer, USA) via tail vein. Tumor volume was assessed weekly for 9 weeks with the following protocol described previously (*20*). Tumor burden was determined by measuring the surface of the largest thyroid cross section normalized to the size of the gland at the beginning of the study. In this model of thyroid cancer, all thyrocytes are undergoing molecular changes leading to cancerization of the entire thyroid gland. Therefore, the assessment of whole thyroid size for tumor burden is a reliable and well-accepted approximation (*9*,*21*,*23*).

Statistical Analysis

A two-way ANOVA test was performed to evaluate the difference in tumor burden measurement between treatment groups. A one-way ANOVA test was used to evaluate the difference in *NIS* mRNA levels *in vitro,* radioiodine uptake *in vivo*, and differences *in vivo* between treatments on mRNA levels of different genes (followed by Tukey's multiple comparisons test). All statistical analyses were performed using Graphpad Prism. P-values equal to or less than 0.05 were considered significant.

RESULTS

MEK Inhibition Alone or in Combination with PI3'K Inhibition Enhances *NIS* mRNA Transcription and Increases Intracellular Iodine Transport *in Vitro*

The effect of the MEK inhibitor PD-325901 and BRAF inhibitor PLX-4032 (vemurafenib) alone or combined with the PI3'K inhibitor GDC-0941 was evaluated on mRNA transcription levels of *NIS* in 8505c and OCUT-2, two ATC cell lines harboring a $BRAF^{V600E}$ mutation (Figure 2A). In 8505c, PD-325901 treatment alone induced a 4-fold increase in *NIS* mRNA level after 48 h, the addition of GDC-0941 did not further augment *NIS* mRNA expression. GDC-0941 alone did not have an effect on *NIS* transcription, and PLX-4032 did not lead to a significant elevation of *NIS* mRNA expression when it was applied alone or in combination with GDC-0941. Treatment of the OCUT-2 cell line, which has a $PIK3CA^{H1047R}$ mutation in addition to a $BRAF^{V600E}$ mutation, showed similar upregulation of *NIS* mRNA transcription following treatment with PD-325901, with an additional response to GDC-0941 alone (3-fold increase in *NIS* mRNA level) and with the

combination of PD-325901 and GDC-0941 (9-fold increase). In OCUT-2, PLX-4032 alone or in combination with GDC-0941 resulted in a 5-fold increase in *NIS* mRNA levels.

Following 48 h treatment with PD-325901 at varying concentrations ranging from 0 to 1 μM, cellular iodine uptake increased by more than double in OCUT-2 and 8505c, as well as in SW1736, a third ATC cell line also harboring a $BRAF^{V600E}$ mutation. Addition of 200 nM GDC-0941 with PD-325901 further increased uptake of ^{123}I in the OCUT-2 and SW1736 cell lines, but not in 8505c (Figure 2B).

MEK Inhibition but not $BRAF^{V600E}$ Inhibition Increases *Nis*, *Tshr*, *Tg*, *Pax8*, and *Tpo* mRNA Transcription *in Vivo*, Which Correlates with Histological Re-normalization of Thyroid Follicles.

A four-fold increase in *Nis* mRNA levels extracted from formalin-fixed, paraffin-embedded tumor sections in $BRAF^{V600E}$ single mutant mice (*21*) treated with the MEK inhibitor PD-325091 as compared to control mice (Figure 3A) was observed. Additionally, the treated group showed restoration of normal thyroid follicular structure (near spheroid follicles containing colloid substance) on H&E staining (Figure 3B), while the control group displayed a papillary structure and absence of normal thyroid follicles.

We then switched to a more aggressive murine $BRAF^{V600E}$ $PIK3CA^{H1047R}$ double mutant model. In animals treated with the MEK inhibitor PD-325901, there was upregulation of *Nis* mRNA by almost 20-fold. The selective $BRAF^{V600E}$ inhibitor PLX-4720 did not increase *Nis* mRNA transcription, nor did the PI3'K inhibitor GDC-0941 alone or in combination with PD-325901 or PLX-4720 (Figure 3C).

Evaluation of mRNA transcription of additional genes known to be important in thyroid gland function was performed, including *Tshr*, *Pax8*, *Tg*, *Tpo* and *Ttf1*. For all genes except *Ttf-1*,

the same pattern as *Nis* was observed with a strong response to PD-325901, no further elevation in combination with GDC-0941 and little response to any of the other drugs alone (Figure 3C). Elevation of protein expression could be confirmed in IHC for TG, PAX8 and TTF-1 (Sup Fig 1).

Increased *Nis, Tshr, Tg, Pax8* and *Tpo* transcription correlated with histological near-normalization in the appearance of thyroid follicles after 10 days of PD-325901 treatment on H&E, a finding that was not replicated in control mice or mice treated with PLX-4720, GDC-0941 (Figure 3D).

MEK Inhibition Leads to a Significant Increase in Thyroid Radioiodine Uptake in BRAF^{V600E} PIK3CA^{H1047R} Double Mutant Mice.

ollowing gene expression analyses, a validation of functional changes in in radioiodine uptake in BRAF^{V600E} PIK3CA^{H1047R} double mutant mice using PD-325901 alone and in combination with GDC-0941 was attempted. After 14 days of daily treatment with PD-325901 with or without GDC-0941, there was a 2.5-fold increase in ^{125}I thyroid uptake in BRAF^{V600E} PIK3CA^{H1047R} double mutant mice compared with controls. There was no significant difference in thyroid radioiodine uptake between mice treated with PD-325901 or those treated with a combination of PD-325901 and GDC-0941. Liver uptake, used to assess background uptake due to passive diffusion through the apical membrane, remained stable across the different treatment regimens. The level of ^{125}I in the blood was approximately 15% injected dose per gram and did not significantly change with the different treatments. The salivary glands, which express NIS but are not able to store iodine due to lack of TG expression, showed slightly decreased uptake with combination treatment (Figure 4).

MEK Inhibitor Treatment Prior to ^{131}I Therapy Reduce Tumor Burden in BRAF^{V600E} PIK3CA^{H1047R} Double Mutant Mice.

An evaluation of the translation from the observed increase in radioiodine uptake in BRAF^{V600E} PIK3CA^{H1047R} double mutant mice treated with MEK inhibition via PD-325901 into reduced tumor burden when injected with therapeutic radioiodine (^{131}I) was performed. The treatment study design including tumor induction, treatment with PD-325901 and radioiodine therapy is depicted in Figure 5A. The control group displayed progressive tumor growth of approximately 15% each week. Mice receiving a 10-day course of treatment with PD-325901 only experienced an initial reduction in tumor burden, with the therapeutic effect disappearing immediately after treatment cessation. The group of mice injected with radioiodine alone demonstrated a stable tumor burden for 6 weeks before tumors eventually increased in size. Mice treated with a 10-day course of PD-325901 followed by injection with ^{131}I displayed a reduction in the tumor burden by 60% of the initial size 6 weeks after iodine injection and remained stable for 3 weeks (Figure 5B).

DISCUSSION

Important genes in thyroid hormone synthesis such as *NIS*, *TSHR*, *TG* and *TPO* are frequently downregulated in advanced thyroid cancer. The loss of this machinery is progressive, beginning with NIS then involving TPO, TG and TSHR (*24–26*).

In the present study, we showed *in vitro* evidence that MEK inhibition induced robust *NIS* mRNA transcription in human ATC cell lines harboring a BRAF^{V600E} mutation, which resulted in elevated cellular ^{123}I uptake. We also showed that this result could be translated *in vivo* in a

mouse model of lethally aggressive thyroid cancer by significantly elevating the radioiodine uptake resulting in stable reduction of tumor burden.

We have previously shown that MEK inhibition in combination with PI3'K inhibition could lead to profound reduction driven by apoptosis (*27*). This treatment, while promising, has the disadvantage of synergistic side effects associated with both drugs. Moreover, after treatment cessation, a rapid regrowth of tumors occurred. In the present study, a short period of drug treatment (10 days) enabled a potentially curative treatment with radioiodine.

In vivo, MEK inhibition in a $BRAF^{V600E}$ single mutant mouse model resulted in a *Nis* 4-folds transcription elevation (Figure 3A). This iodine induction in a PTC model is consistent with the current literature (*13*,*28*,*29*). In a mouse model of more advanced thyroid cancer harboring $BRAF^{V600E}$ and $PIK3CA^{H1047R}$ mutations (Figure 3C), we demonstrated that a MEK inhibition induced a strong elevation of mRNA levels of genes important in thyroid hormones synthesis, such as *Nis* (6-folds), *Tshr*, *Tg, Pax8 and Tpo*. Interestingly, the combination of MEK inhibition with PI3'K inhibition did not provide further upregulation of the tested genes. Specific $BRAF^{V600E}$ inhibition did not induce an increase in any of these transcripts (Figure 3C). This is concordant with Nagarajah and colleagues, who showed that the more profound MEK inhibition is achieved, the stronger the NIS re-expression (*29*). It was previously demonstrated that BRAF specific inhibition can induce only transient ERK de-phosphorylation and the signal is restored with time through the wildtype allele of BRAF (*30*). Additionally, our recent findings show that $BRAF^{V600E}$-specific inhibition led to a paradoxical activation of ERK in the double mutant mouse model (*20*). Furthermore, there are very few data reporting vemurafenib treatment in ATC and one showed mitigated results including one progression under $BRAF^{V600E}$ inhibitor (*31*).

On a functional level, a nearly 2.5-fold increase in radioiodine uptake in the thyroids of mice treated with a MEK inhibitor as compared to mice receiving the control treatment was observed (Figure 4) after only 10 days of PD-325901 treatment. Increased radioiodine uptake translated into a stable, profound reduction in tumor burden (Figure 5). Mice treated with radioiodine showed only an initial stabilization of the tumor burden followed by a rapid tumor growth. This short-lasting response to radioiodine could be explained by tumor heterogeneity with regions of untransformed cells and PTC. As there was no added benefit of using a drug combination with a PI3'K inhibitor even in tumors harboring a $PIK3CA^{H1047R}$ mutation (Figure 4), this was not tested in the context of curative radioiodine.

In conclusion, our study shows that MEK inhibition as a single-drug treatment is the most efficient regimen to induce the expression of protein machinery required for iodine uptake in human ATC cell lines and in our aggressive murine model of thyroid cancer. Until now, most studies have mainly focused on PTC mouse models driven by a single $BRAF^{V600E}$ mutation (*13*). Here we provide new evidence that the RAS-MEK-ERK axis is essential for NIS expression even in ATC cell lines and in a clinically relevant mouse model carrying the two mutations $BRAF^{V600E}$ and $PIK3CA^{H1047R}$. We performed a meta-analysis of the three available studies conducting genetic profiling in ATC patients, which showed that the occurrence of both BRAF and PIK3CA mutations is found in 12% of ATC patients (supplementary table and (*5*–*7*)). Thus, we believe that the present results represent an encouraging initial step toward the successful treatment of non-radioiodine responsive thyroid cancers.

ACKNOWLEDGEMENTS

We thank Prof. Martin McMahon for his mentorship and for providing the BRAF mutant mice. We thank Prof. Engelhard, Dr. Deutsch and Dr. Benarafa for permission to use the vivarium at the Theodor Kocher Institute. We would also like to thank Dr. Colin for his help with Figure 1. Also, we acknowledge the Microscopy Imaging Center of the University of Bern (MIC) for their contributions to this study. Oussama ElMokh and Matthias Roelli were enrolled in the Graduate School for Cellular and Biomedical Research (GCB) of the University of Bern during this study.

REFERENCES

1. Kebebew E, Greenspan FS, Clark OH, Woeber KA, McMillan A. Anaplastic thyroid carcinoma. Treatment outcome and prognostic factors. *Cancer*. 2005;103:1330-1335.

2. Gilliland FD, Hunt WC, Morris DM, Key CR. Prognostic factors for thyroid carcinoma: A population-based study of 15,698 cases from the Surveillance, Epidemiology and End Results (SEER) program 1973-1991. *Cancer*. 1997;79:564-573.

3. Mazzaferri EL. An overview of the management of papillary and follicular thyroid carcinoma. *Thyroid*. 1999;9:421-427.

4. Kim EK, Choi E. Biochimica et Biophysica Acta Pathological roles of MAPK signaling pathways in human diseases. *BBA - Mol Basis Dis*. 2010;1802:396-405.

5. Kunstman JW, Christofer Juhlin C, Goh G, et al. Characterization of the mutational landscape of anaplastic thyroid cancer via whole-exome sequencing. *Hum Mol Genet*. 2015;24:2318-2329.

6. Pozdeyev N, Gay LM, Sokol ES, et al. Genetic analysis of 779 advanced differentiated and anaplastic thyroid cancers. *Clin Cancer Res*. 2018.

7. Landa I, Ibrahimpasic T, Boucai L, et al. Genomic and transcriptomic hallmarks of poorly differentiated and anaplastic thyroid cancers. *J Clin Invest*. 2016;126:1052-1066.

8. Xing M. Molecular pathogenesis and mechanisms of thyroid cancer. *Nat Rev Cancer*. 2013;13:184-199.

9. Charles R-P, Silva J, Iezza G, Phillips WA, McMahon M. Activating BRAF and PIK3CA Mutations Cooperate to Promote Anaplastic Thyroid Carcinogenesis. *Mol Cancer Res*. 2014;12:979-986.

10. Riesco-Eizaguirre G, Gutiérrez-Martínez P, García-Cabezas M, Nistal M, Santisteban P. The oncogene BRAFV600E is associated with a high risk of recurrence and less differentiated papillary thyroid carcinoma due to the impairment of Na+/I- targeting to the membrane. *Endocr Relat Cancer*. 2006;13:257-269.

11. Romei C, Ciampi R, Faviana P, et al. BRAFV600E mutation, but not RET/PTC rearrangements, is correlated with a lower expression of both thyroperoxidase and sodium iodide symporter genes in papillary thyroid cancer. *Endocr Relat Cancer*. 2008;15:511-520.

12. Costamagna E, García B, Santisteban P. The Functional Interaction between the Paired Domain Transcription Factor Pax8 and Smad3 Is Involved in Transforming Growth Factor-β Repression of the Sodium/Iodide Symporter Gene. *J Biol Chem*. 2004;279:3439-3446.

13. Chakravarty D, Santos E, Ryder M, et al. Small-molecule MAPK inhibitors restore radioiodine incorporation in mouse thyroid cancers with conditional BRAF activation. *J Clin Invest*. 2011;121.

14. Liu Y-Y, Zhang X, Ringel MD, Jhiang SM. Modulation of sodium iodide symporter expression and function by LY294002, Akti-1/2 and Rapamycin in thyroid cells. *Endocr Relat Cancer*. 2012;19:291-304.

15. Bozorg-Ghalati F, Hedayati M, Dianatpour M, Azizi F, Mosaffa N, Mehrabani D. Effects of a Phosphoinositide-3-Kinase Inhibitor on Anaplastic Thyroid Cancer Stem Cells. *Asian Pac J Cancer Prev*. 2017;18:2287-2291.

16. Shah N, Iyer RM, Mair H-JJ, et al. Improved human bioavailability of vemurafenib, a practically insoluble drug, using an amorphous polymer-stabilized solid dispersion

prepared by a solvent-controlled coprecipitation process. *J Pharm Sci*. 2013;102:967-981.

17. Dankort D, Filenova E, Collado M, Serrano M, Jones K, McMahon M. A new mouse model to explore the initiation, progression, and therapy of BRAFV600E-induced lung tumors. *Genes Dev*. 2007;21:379-384.

18. Kinross KM, Montgomery KG, Kleinschmidt M, et al. An activating Pik3ca mutation coupled with Pten loss is sufficient to initiate ovarian tumorigenesis in mice. *J Clin Invest*. 2012;122:553-557.

19. Undeutsch H, Löf C, Offermanns S, Kero J. A mouse model with tamoxifen-inducible thyrocyte-specific cre recombinase activity. *Genesis*. 2014;52:333-340.

20. Roelli MA, Ruffieux-Daidié D, Stooss A, et al. PIK3CAH1047R-induced paradoxical ERK activation results in resistance to BRAFV600E specific inhibitors in BRAFV600E PIK3CAH1047R double mutant thyroid tumors. *Oncotarget*. 2017;8:103207-103222.

21. Charles RP, Iezza G, Amendola E, Dankort D, McMahon M. Mutationally activated BRAFV600E elicits papillary thyroid cancer in the adult mouse. *Cancer Res*. 2011;71:3863-3871.

22. Haura EB, Ricart AD, Larson TG, et al. A phase II study of PD-0325901, an oral MEK inhibitor, in previously treated patients with advanced non-small cell lung cancer. *Clin Cancer Res*. 2010;16:2450-2457.

23. McFadden DG, Vernon A, Santiago PM, et al. p53 constrains progression to anaplastic thyroid carcinoma in a Braf-mutant mouse model of papillary thyroid cancer. *Proc Natl Acad Sci*. 2014;111:E1600--E1609.

24. Lazar V, Bidart JM, Caillou B, et al. Expression of the Na+/I- symporter gene in human

thyroid tumors: A comparison study with other thyroid-specific genes. *J Clin Endocrinol Metab*. 1999;84:3228-3234.

25. Gérard AC, Daumerie C, Mestdagh C, et al. Correlation between the Loss of Thyroglobulin Iodination and the Expression of Thyroid-Specific Proteins Involved in Iodine Metabolism in Thyroid Carcinomas. *J Clin Endocrinol Metab*. 2003;88:4977-4983.

26. Russo D, Damante G, Puxeddu E, Durante C, Filetti S. Epigenetics of thyroid cancer and novel therapeutic targets. *J Mol Endocrinol*. 2011;46.

27. Elmokh O, Ruffieux-daidié D, Roelli MA, et al. Combined MEK and Pi3 ' -kinase inhibition reveals synergy in targeting thyroid cancer in vitro and in vivo. *Oncotarget*. 2017;8:24604-24620.

28. Ho AL, Grewal RK, Leboeuf R, et al. Selumetinib-enhanced radioiodine uptake in advanced thyroid cancer. *N Engl J Med*. 2013;368:623-632.

29. Nagarajah J, Le M, Knauf JA, et al. Sustained ERK inhibition maximizes responses of BrafV600E thyroid cancers to radioiodine. *J Clin Invest*. 2016;126:4119-4124.

30. Hatzivassiliou G, Song K, Yen I, et al. RAF inhibitors prime wild-type RAF to activate the MAPK pathway and enhance growth. *Nature*. 2010;464:431-435.

31. Hyman DM, Puzanov I, Subbiah V, et al. Vemurafenib in Multiple Nonmelanoma Cancers with BRAF V600 Mutations. *N Engl J Med*. 2015;373:726-736.

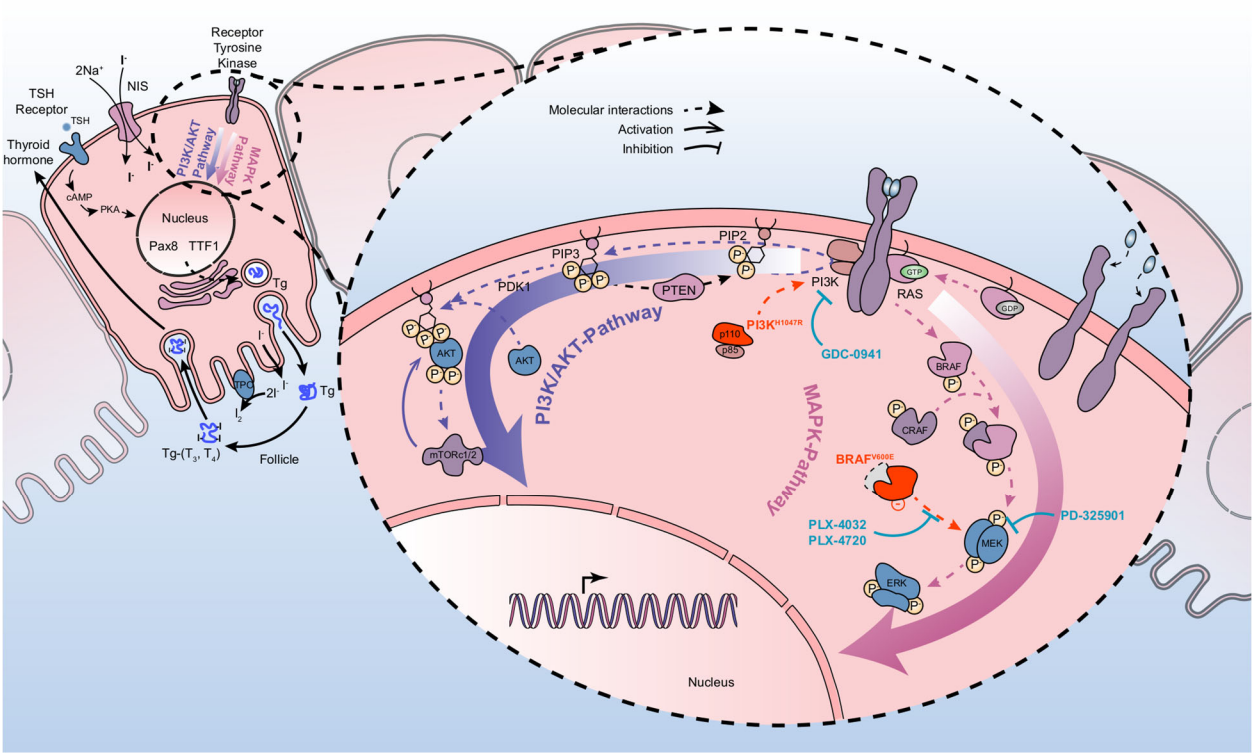

Figure 1: Mutationally activated pathways in the mouse model of thyroid cancer used.

(Left) Schematic illustration of a thyrocyte depicting the key aspects of thyroid iodine transport and thyroid hormone synthesis:

Iodide (I^-) uptake is the first and rate-limiting step in the biosynthesis of thyroid hormone and is mediated by the sodium iodide symporter (NIS). Iodide is oxidized to iodine (I_2) by tyrosine peroxidase (TPO), that incorporates iodine into tyrosyl residues along the thyroglobulin (Tg) backbone in the colloid substance. Thyroglobulin fragments coupled to thyroid hormone enter the thyrocyte by pinocytosis. Cleavage by endopeptidases results in release of T3 and T4 into the blood. The thyroid-stimulating hormone (TSH) via its receptor stimulates these steps through activation of the cAMP-PKA pathway and the regulation of several transcription factors directly involved in thyroid hormone synthesis, such as PAX8 and TTF-1.

(Right) Schematic illustration of the MAPK and PI3'K pathways, including relevant mutations and drug targets in thyroid cancer.

The MAPK and PI3'K pathways are involved in cellular proliferation and differentiation, and activation of these pathways drives cell growth and decreases iodine metabolism. The mutation $BRAF^{V600E}$ (in red) stimulates the MAPK pathway independent of the upstream signal. The activation of RAS through binding of an extracellular ligand to a receptor tyrosine kinase leads to activation of PI3'K. From PIP3, a phosphate is transferred to 3-phosphoinositide-dependent protein kinase 1 (PDK1) which in turn phosphorylates AKT, leading to its activation and translocation into the nuclei, where it regulates transcription of target genes involved in growth. P-AKT in the cytoplasm activates other targets such as the mammalian target of rapamycin (mTOR) which is important in promoting proteins translation and consequently cell growth. PTEN is a phosphatase converting PIP3 to PIP2 and playing the role of tumor suppressor as major negative regulatory mechanism of the PI3'K/AKT pathway. The mutation $PI3KCA^{H1047R}$ results in the hyperactivation of the pathway. Pharmacological inhibition of $BRAF^{V600E}$ occurs with PLX-4032/vemurafenib or PLX-4720, a pre-clinical analog. MEK is specifically inhibited by PD-325901, which leads to inhibition of ERK activity. PI3'K is specifically inhibited by GDC-0941.

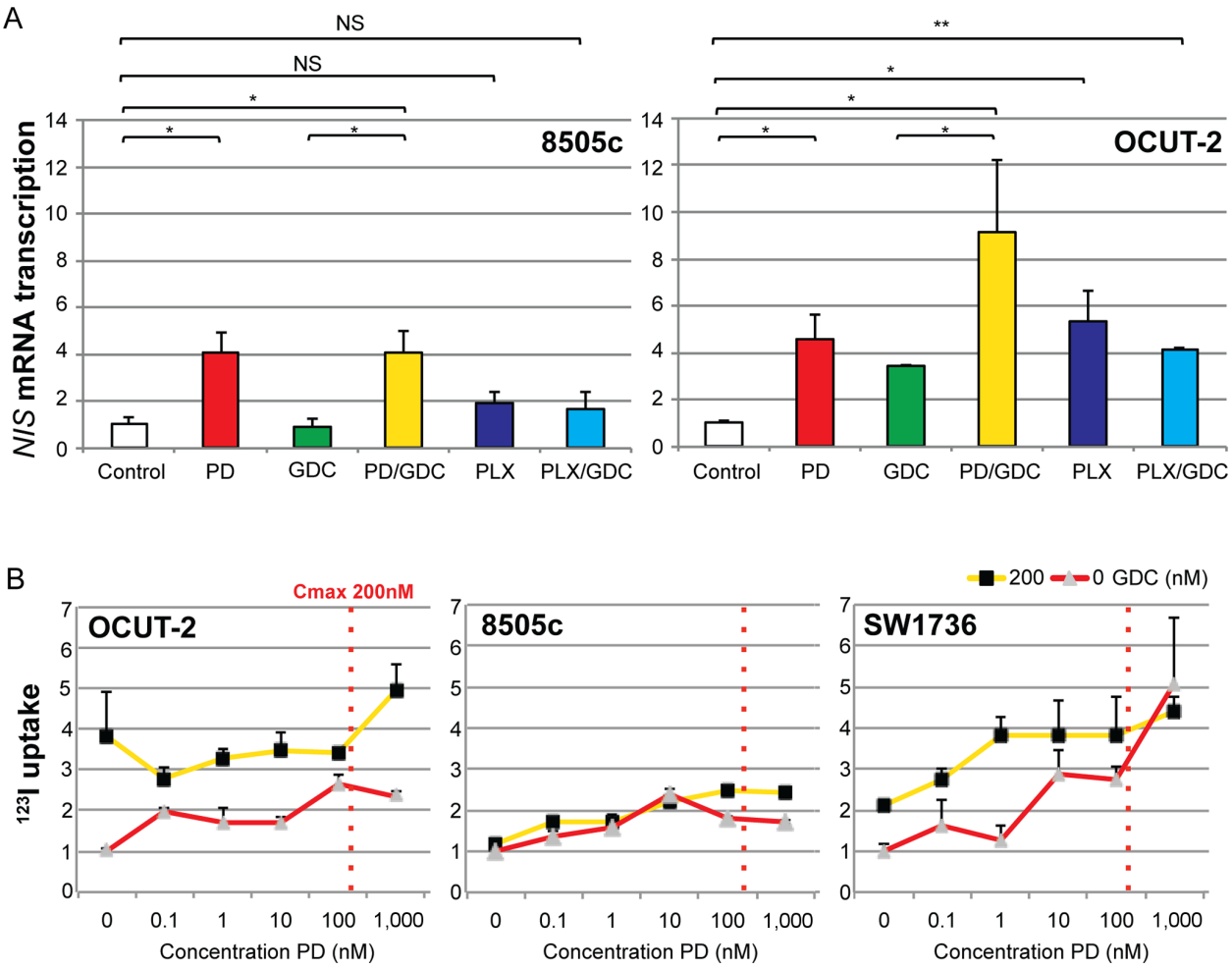

Figure 2: MEK inhibition lead to an elevation of *NIS* mRNA levels and iodine uptake *in vitro.*

(A) *NIS* mRNA levels in 2 ATC cell lines 8505c and OCUT-2 treated for 48 h with PD at 100 nM alone, PLX at 1 µM alone, or in combination with GDC at 1 µM. Values are normalized to untreated cells. (B) ^{123}I uptake in 3 ATC cell lines treated with different concentrations of PD alone or in combination with GDC. Values are normalized to untreated cells. C_{max} indicates the maximum plasma concentration of PD in patients without side effects.

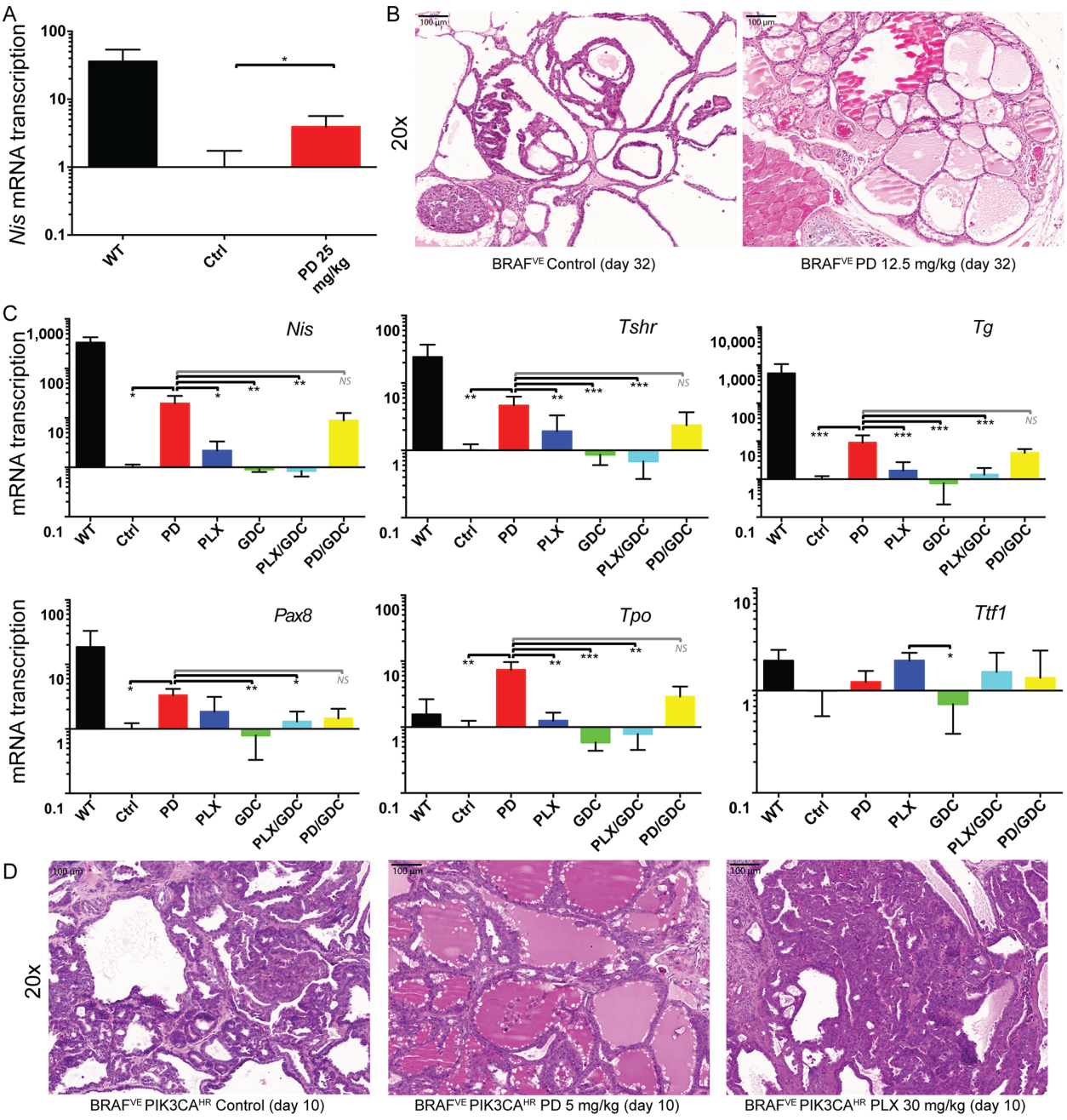

Figure 3: MEK inhibition but not BRAF^{V600E} inhibition induced a restoration of *Nis*, *Tshr* and *Tg* transcripts and resulted in near-normalization of follicular organization *in vivo*.

(A) *NIS* mRNA levels in BRAF^{V600E} single mutant mice treated with PD or control. (B) H&E stained thyroid sections. (C) mRNA expression levels of *Nis*, *Tshr*, *Tg*, *Pax8*, *Tpo* and *Ttf1* normalized to normal levels in double mutant mice (BARF^{V600E} PIK3CA^{H1047R}) treated with control, PD, PLX , or

GDC, PLX/GDC or PD/GDC for 10 days. (D) H&E stained thyroid sections from mice after treatments.

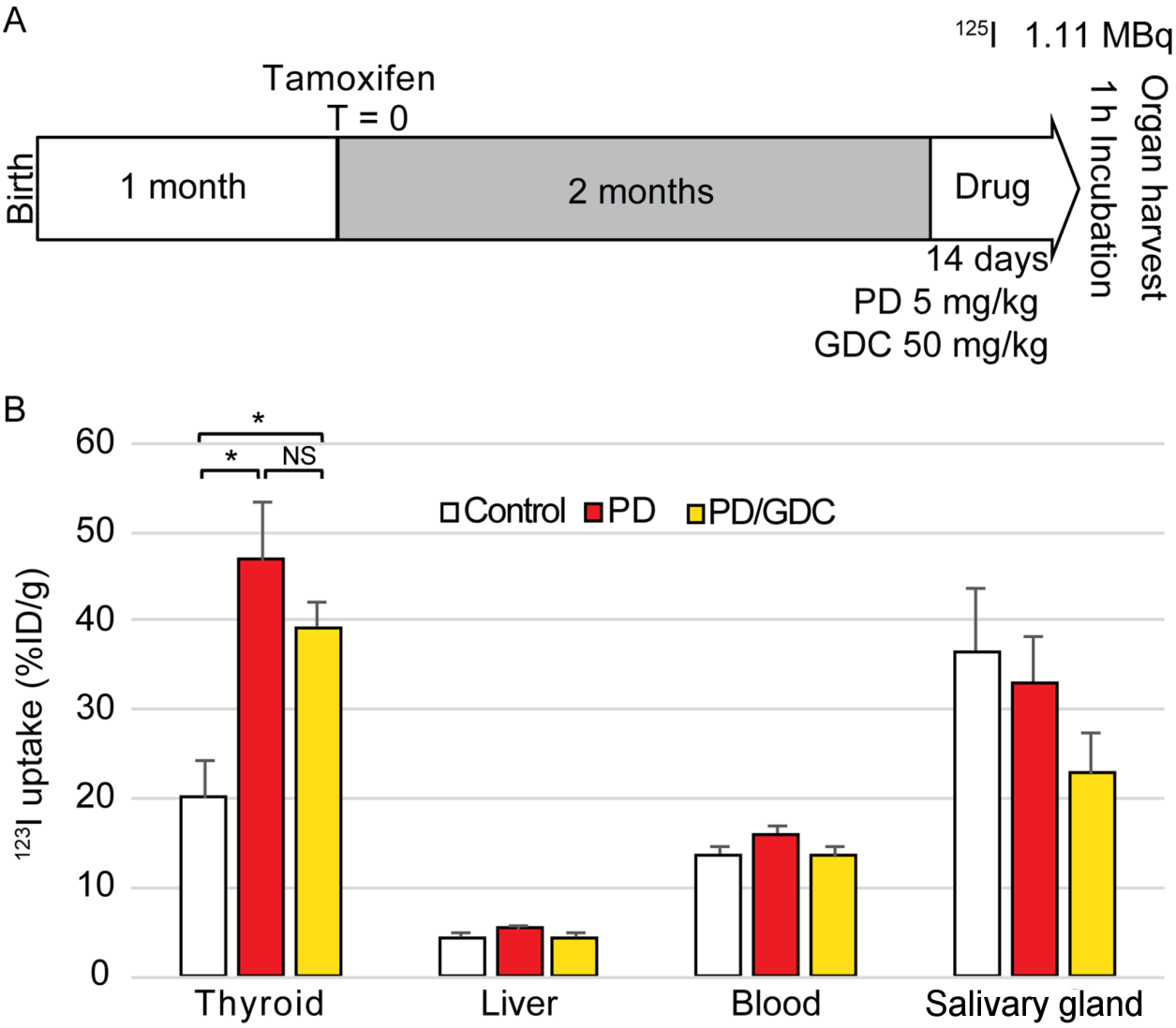

Figure 4: MEK inhibition lead to increased radioactive iodine uptake by the thyroid in BRAF^{V600E} PIK3CA^{H1047R} double mutant mice.

(A) Schematic representation of the *in vivo* radioiodine uptake experiment. (B) Uptake expressed as percent injected dose of ^{125}I per gram of tissue in the thyroid, salivary glands, liver and blood harvested from mice treated with control, PD alone or in combination with GDC for 2 weeks.

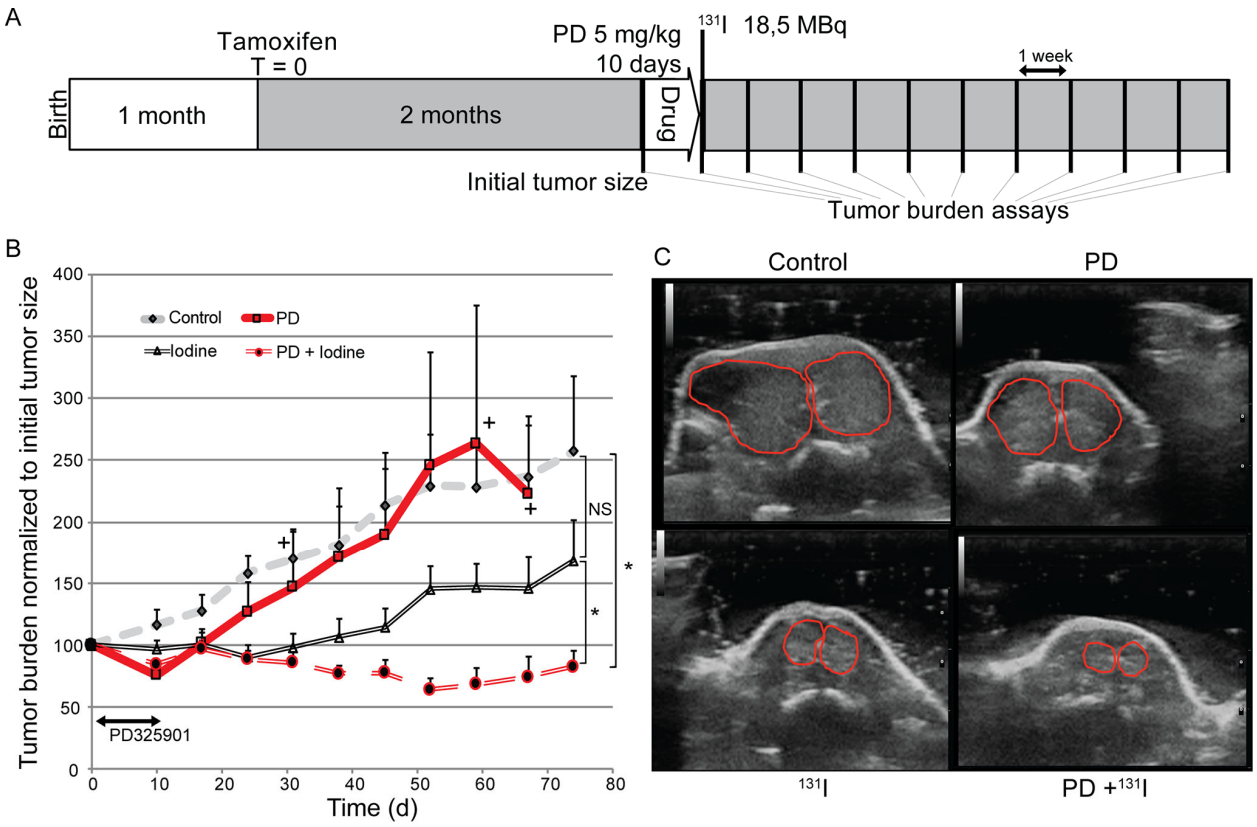

Figure 5: Combination of MEK inhibition with ^{131}I lead to a profound reduction in tumor burden in BRAF^{V600E} PIK3CA^{H1047R} double mutant mice.

(A) Schematic representation of the *in vivo* treatment study. (B) Thyroid tumor burden measured weekly by ultrasound expressed as percentage of the pretreatment tumor burden in mice (C) Representative grayscale ultrasound images of the thyroid gland at 77 days after treatment from mice in the 4 different treatment cohorts.

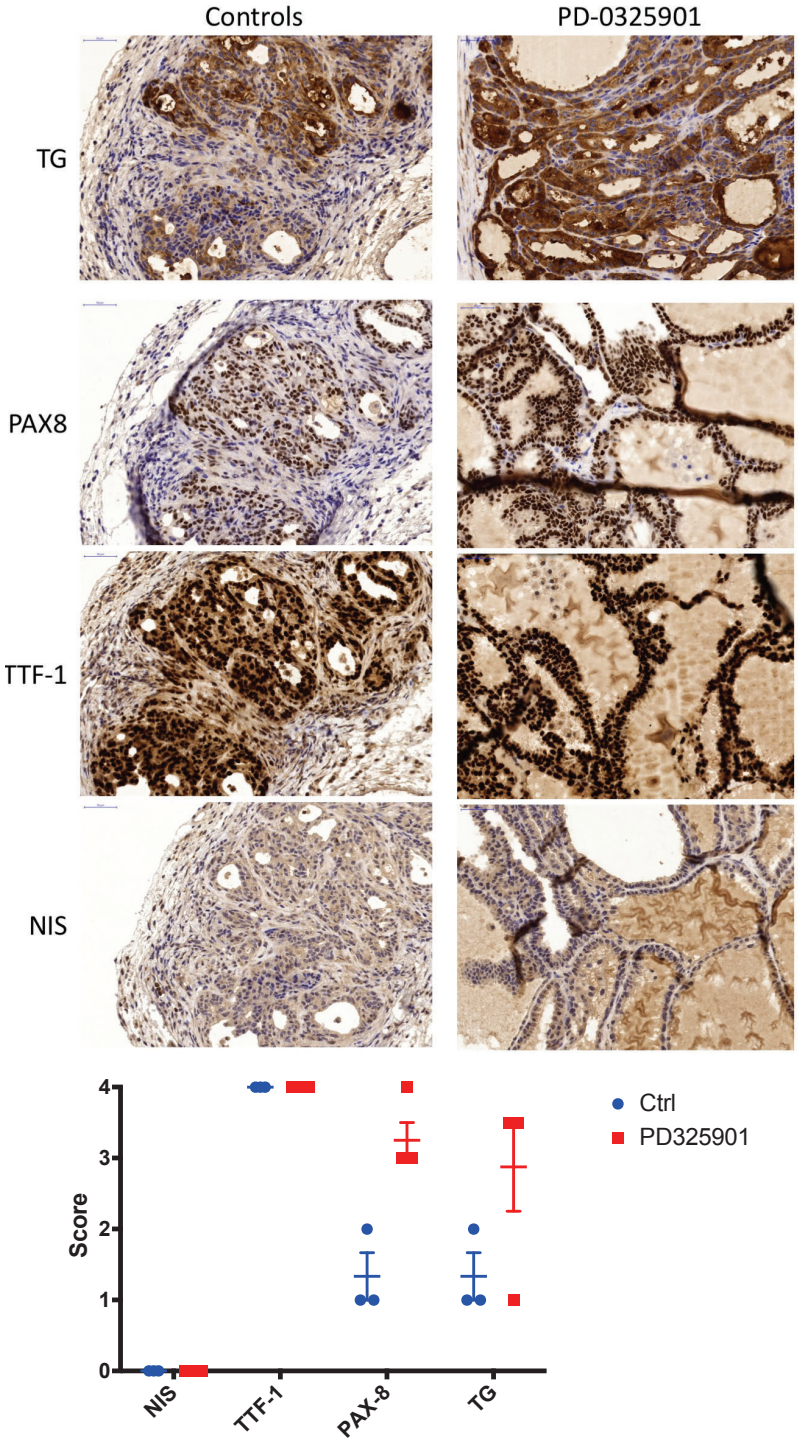

Supplementary figure 1:
Upper panel: IHC for Thyroglobulin (TG), PAX-8, Thyroid transcription factor 1 (TTF-1) and Sodium iodine symporter (NIS) on thyroid tissues treated for 10 days with 5 mg/kg of PD-0325901.
Lower Panel: Score of the depicted IHC, individual values with mean and SEM (0= Negative, 1=weak positive, 2=Positive, 3=strongly positive, 4=very strong positive).

Supplementary Material and Methods:

IHC stains were obtained by automatized stainings with a Leica immunostainer following the protocol described here: Berezowska S, Galván JA. Methods Mol Biol. 2017;1560:189-194. doi: 10.1007/978-1-4939-6788-9_13. PMID: 28155154.

The following antibodies and specific conditions were used:

Antibody	Dilution	Antigen retrieval	Host	incubatin time	Polymer	DAB chromogen(*)	Comany	Ref. Number
TG	1:10000	Tris buffer 30 min 95º	Rb	15min	8min	8min	Dako	A0251
PAX8	1:1200	Tris buffer 30 min 95º	Rb	15min	8min	8min	Proteintech	10336-1-AP
TTF1	1:50	Tris buffer 30 min 95º	Rb	30min	15min	10min	Santa Cruz	sc-13040
NIS	1:50	Tris buffer 30 min 95º	Rb	30min	15min	10min	Abbiotec	250552
Visualization Kits								
Bond Polymer		Leica Biosystems	DS9800					
Refine Detection (*)								
Autostainer								
Leica BOND RX		Leica Biosystems						

	total (ATC)	BRAF	frequency	PI3K	frequency	BRAF/PI3K	frequency
Pozdeyev et al.	196	84	43%	29	15%	23	12%
Kunstman et al.	22	6	27%	2	9%	2	9%
Landa et al.	33	15	45%	6	18%	5	15%
TOTAL	**251**	**105**	**42%**	**37**	**15%**	**30**	**12%**

Supplementary table 1:

Analysis of BRAF and PI3K mutations occurrence in thyroid cancers.

Data extracted from:

Pozdeyev N, Gay LM, Sokol ES, et al. Genetic analysis of 779 advanced differentiated and anaplastic thyroid cancers. Clin Cancer Res. 2018.

Landa I, Ibrahimpasic T, Boucai L, et al. Genomic and transcriptomic hallmarks of poorly differentiated and anaplastic thyroid cancers.

J Clin Invest. 2016 and Kunstman JW, Christofer Juhlin C, Goh G, et al. Characterization of the mutational landscape of anaplastic thyroid cancer via whole-exome sequencing. Hum Mol Genet. 2015.

The Journal of NUCLEAR MEDICINE

MEK inhibition induces therapeutic iodine uptake in a murine model of anaplastic thyroid cancer.

Oussama ElMokh, Vincent Taelmann, Piotr Radojewski, Matthias Andreas Roelli, Amandine Stooss, Rebecca A Dumont, Matthias Dettmer, Wayne Phillips, Martin Alexander Walter and Roch-Philippe Régis Charles

J Nucl Med.
Published online: November 21, 2018.
Doi: 10.2967/jnumed.118.216721

The Journal of Nuclear Medicine is published monthly.
SNMMI | Society of Nuclear Medicine and Molecular Imaging
1850 Samuel Morse Drive, Reston, VA 20190.
(Print ISSN: 0161-5505, Online ISSN: 2159-662X)

SNMMI SOCIETY OF NUCLEAR MEDICINE AND MOLECULAR IMAGING